Tunable Bands of Electronic Image States in Nanowire Lattices

Dvira Segal,[1,2] Brian E. Granger,[3] H. R. Sadeghpour,[4] Petr Král,[1,2] and Moshe Shapiro[1,2]

[1]*Department of Chemical Physics, Weizmann Institute of Science, 76100 Rehovot, Israel*
[2]*Department of Chemistry, University of British Columbia, Vancouver, Canada V6T1Z1*
[3]*Department of Physics, Santa Clara University, Santa Clara, California 95053, USA*
[4]*ITAMP, Harvard-Smithsonian Center for Astrophysics, Cambridge, Massachusetts 02138, USA*

(Received 16 April 2004; published 3 January 2005)

We demonstrate that suspended arrays of parallel nanowires support bound electron image states with rich *band structures*. Surprisingly, these Bloch states can be highly detached from the surfaces of the nanowires, similar to the single-tube wave functions. This is because an electron hovering in such a *periodic* lattice of nanowires is influenced by a Coulombic-like attraction and a centrifugal repulsion, which are both *central symmetric* around each wire. These novel states could be used in building of waveguides, mirrors, and storage places for Rydberg-like electrons.

DOI: 10.1103/PhysRevLett.94.016402 PACS numbers: 71.20.–b, 34.60.+z, 36.10.–k, 61.46.+w

Dielectric materials with periodic structures formed in biological systems can efficiently filter and guide light [1]. Based on the same principles, man-made "photonic band-gap" materials [2] have been designed to propagate photons, much the same way crystalline solids propagate electrons, promising revolutionary advances in optics. Light can also be guided in arrays of circular rods [3] and carbon nanotubes [4]. Interestingly, similar metallic arrays can even hold ultracold matter [5].

Recently, we have shown that a suspended nanowire, such as a metallic carbon nanotube, can support electronic image states that are highly detached from its surface [6]. These "tubular image states" (TIS), which resemble very stable molecular Rydberg states [7], owe their stability to the balance between the Coulombic-like attraction and the centrifugal repulsion associated with the circular motion of the electron around the nanowire. We have examined TISs in electric and magnetic fields and calculated their angular-momentum relaxation times $\tau_l \approx 1$–100 ns, due to scattering with flexural phonon modes of the tube [8]. The TISs have been recently observed experimentally and their properties found to be in agreement with theoretical predictions [9].

From the point of practical applications, it is crucial to examine the existence of Rydberg-like image states in *periodic arrays* of nanowires [10]. These Bloch states could resemble light states in photonic band-gap systems or atomic matter waves formed in optical lattices [11]. In this work, we explore this attractive idea in a system composed of an array of metallic nanotubes surrounded by the electron image states, as schematically shown in Fig. 1. The tubes are aligned along the z direction, with their axes placed at the $x = pd$ and $y = qd$ positions ($p, q = 0, \pm 1, \pm 2, \ldots$; with $q = 0$, for a 1D array). Typically, $d/a = 10$–100 gives the ratio of the lattice constant d with the tube radius $a \approx 1$ nm.

We start the discussion by recalling [6] the electrostatic interaction between an electron of charge e, positioned at a distance ρ relative to the center of a single nanowire. Treating it as a perfectly conducting cylinder of radius a, the potential energy of the electron is

$$V(\rho) = -\frac{e^2}{\pi a}\sum_{m=-\infty}^{\infty}\int_0^{\infty} dx\,\frac{I_m(x)}{K_m(x)}[K_m(x\rho/a)]^2, \quad (1)$$

where $I_m(x)$ and $K_m(x)$ are, respectively, the regular and irregular modified Bessel functions of argument x and order m. The limiting forms of the potential $V(\rho)$ can be found by expanding $K_m(x)$ for large and small arguments. We can derive an approximate expression,

$$V(\rho) \approx \frac{2e^2}{\pi a}\sum_{n=1,3,5,\ldots}\mathrm{li}[(a/\rho)^n], \qquad \mathrm{li}(x) \equiv \int_0^x \frac{dt}{\ln(t)}, \quad (2)$$

which reasonably reproduces the exact interaction potential [6] but is easier to evaluate numerically.

Let us examine first a nontrivial example of single-electron TIS around *two* metallic nanotubes. The distances from the electron to the tube centers are $\rho_{1,2} = \sqrt{(x \mp d/2)^2 + y^2}$. Without loss of generality, we approxi-

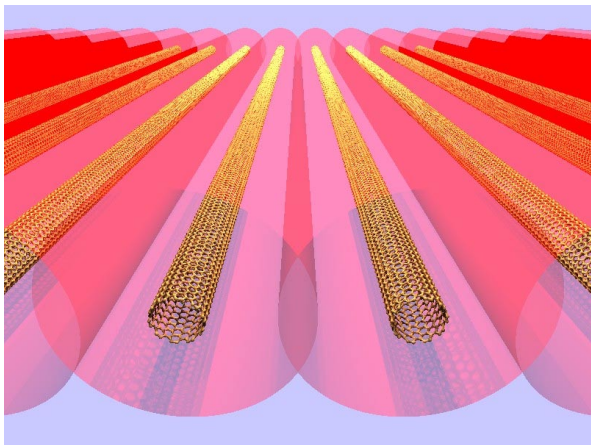

FIG. 1 (color online). Scheme of electron image states formed in the vicinity of a 1D array of parallel metallic nanotubes.

mate the electron-tube interaction by its Coulombic-like form, $V(\rho) = -e^2/4|\rho - a|$, valid close to the tubes. Furthermore, we assume that the total interaction is a sum of the electron's interaction with each nanotube *separately*, $V_T(\rho_1, \rho_2) = V(\rho_1) + V(\rho_2)$. This amounts neglecting the relatively short-range interaction between the induced image charge distributions in the two nanotubes.

The wave functions, $\Psi(x, y, z) = \psi(x, y)\phi(z)$, are separable in the z direction. In the x and y directions, they can be found from the Schrödinger equation, easily solvable in bipolar coordinates, $(x, y) \rightarrow (\xi, \eta)$, given by the transformation $x = b\frac{\sinh(\eta)}{\cosh(\eta)-\cos(\xi)}$, $y = b\frac{\sin(\xi)}{\cosh(\eta)-\cos(\xi)}$. We chose the free parameter $b = a\sinh(\eta_0)$, where $\eta_0 = \cosh^{-1}(d/2a)$ and $a = 0.7$ nm is the radius of the metallic (10, 10) nanotube. Then the tube's exterior spans the ranges $0 \leq \xi \leq 2\pi$ and $-\eta_0 < \eta < \eta_0$.

Since the interaction potential $V_T(\rho_1, \rho_2)$ is symmetric under the reflection about the $\xi = \pi$ and $\eta = 0$ lines (the x and y axes), the states possess a *twofold reflection symmetry*. The $\psi(\xi, \eta)$ wave functions (or their derivatives) thus vanish at $\eta = 0$ and $\xi = \pi$ to generate odd (or even) parity eigenstates. Two parity quantum numbers, $u = \pm$, $v = \pm$, associated with these reflections label the $\psi^{u,v}(\xi, \eta)$ eigenstates and the $E^{u,v}$ eigenenergies.

We obtain them from the Schrödinger equation,

$$-\frac{\hbar^2}{2m_e b^2}(\cosh\eta - \cos\xi)^2\left(\frac{\partial^2}{\partial\eta^2} + \frac{\partial^2}{\partial\xi^2}\right)\psi^{u,v}(\xi, \eta) + V_T(\xi, \eta)\psi^{u,v}(\xi, \eta) = E^{u,v}\psi^{u,v}(\xi, \eta), \tag{3}$$

where m_e is the electron mass. We solve Eq. (3) for the wave functions, $\psi^{u,v}(\xi, \eta) = \sum_{i,j}^{I,J} c_{i,j}^{u,v}\phi_i(\xi)\chi_j(\eta)$, expanded in terms of products of *B splines,* with the expansion coefficients $c_{i,j}^{u,v}$.

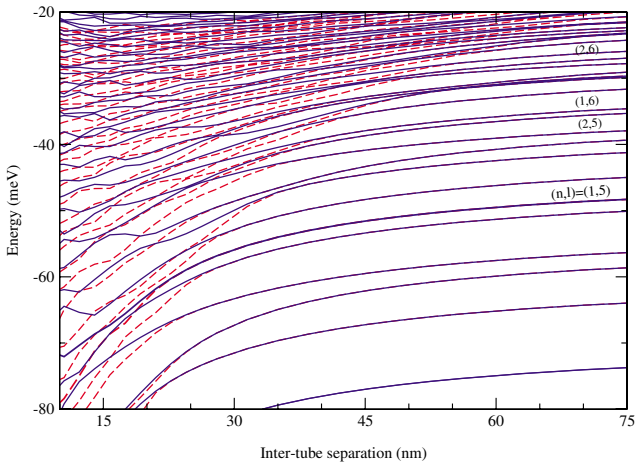

FIG. 2 (color online). Energies of two-tube image states with $u = +$ as a function of intertube separation d. The even ($v = +$, dashed lines) and odd ($v = -$, solid lines) parity-state energies split at small intertube separations. Selected curves are labeled by the quantum numbers (n, l) of the single-tube image potential states to which they converge as $d \rightarrow \infty$.

The calculated $E^{u,v}$ eigenenergies are given in Fig. 2 as a function of the nanotube separation d. At large d, they correspond to energies of electronic wave functions localized over a single tube, which can be numbered by the principal quantum number n and angular momentum l [6]. As the intertube separation decreases, the higher excited single-tube states start to overlap and become gradually modified. The resulting pairs of *degenerate* states split into double-tube states, with even and odd symmetries under the tube exchange ($v = \pm$), in direct analogy to *gerade* and *ungerade* symmetries in molecules. At smaller d, single-tube states with different values of n and l mix, but in some states the number of radial and axial nodes can still be counted. Then level repulsion becomes important and avoided crossings appear.

We also calculate the $\psi^{u,v}(\xi, \eta)$ eigenfunctions and transform them back to the Cartesian (x, y) coordinates. They are chosen to be real, so at large d they correspond to the superposition of the single-tube l and $-l$ states, $\psi_{|l|} \propto \psi_l + \psi_{-l} \propto (e^{-i\phi l} + e^{i\phi l})/2 = \cos(l\phi)$. In Fig. 3, we

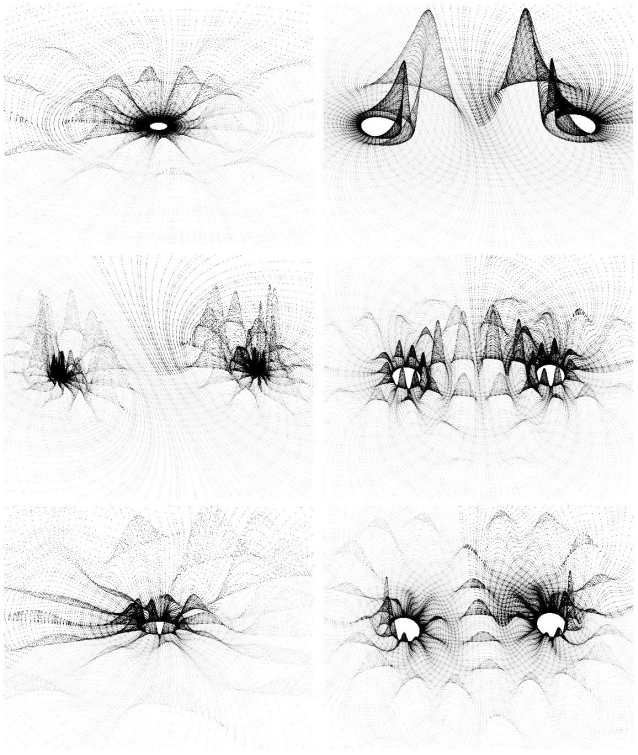

FIG. 3. Left panels: gradual loss of detachment of the $l = 6$, $n = 2$ wave function squared, as the two nanotubes get close: (top) view on one tube for $d = 200a$; (middle) the entire wave function for $d = 80a$; (bottom) detailed view of the right tube in the last case. Right panels: states for much smaller tube separation, $d = 10a$. (top) The modified $l = 0$, $n = 2$ state. (middle) An odd symmetry state with respect to reflection in the y axis. (bottom) An even symmetry state.

present the $|\psi^{u,v}|^2$ densities for several typical wave functions. In the left panels, we demonstrate the evolution of the $l = 6$ and $n = 2$ state. At large tube separations, $d = 200a$ (top panel), it is detached from the tube's surface, similarly as in the single-tube case [6]. At lower but still relatively big separations, $d = 80a$ (middle and bottom panels), this state partially collapses on the tubes, due to *asymmetric distortion* of the attractive potential. The same happens to *all* the single-tube states, as they get closer. We thus expect that their lifetimes should be reduced [6], especially if their energies do not fall in the band gap of the material [12]. In the right panel, we also display more distorted states, obtained for $d = 10a$, showing rather complex nodal structures.

We can proceed to investigate image states of a single electron present in periodic arrays of parallel nanowires. For a 1D array (see Fig. 1), the total potential fulfills $V_T(x, y) = V_T(x + d, y)$. Thus, the transverse Bloch components of the total wave functions $\Psi(x, y, z) = \psi_{m,k}(x, y)\phi_{k_z}(z)$, with energies $\epsilon_{m,k} + E_{k_z}$, fulfill [13]

$$\psi_{m,k}(x, y) = e^{ikx} f_{m,k}(x, y) = e^{ikx} f_{m,k}(x + d, y). \quad (4)$$

They can be obtained from the Schrödinger equation with the Hamiltonian parametrized by k, as

$$\left\{\frac{-\hbar^2}{2m_e}\left[\left(\frac{\partial}{\partial x} + ik\right)^2 + \frac{\partial^2}{\partial y^2}\right] + V_T(x, y)\right\} f_{m,k}(x, y) = \epsilon_{m,k} f_{m,k}(x, y). \quad (5)$$

An analogous equation, with the $\mathbf{k} = (k_x, k_y)$ wave vectors, is used below for a 2D (square) lattice of nanotubes.

We solve Eq. (5) numerically, by a multidimensional discrete variable representation algorithm [14]. We use the single-tube potential (2) and include in V_T the interaction due to the central tube in the cell and its two (1D) or eight (2D) neighbors, while neglecting multiple reflection, as in the two-tube case. The intertube separation is varied between $d = 5$–80 nm and $a = 0.7$ nm. The calculations are done with a grid of spacing Δ for a fixed ratio $\Delta/d \approx 0.0075$. Therefore, results obtained for larger lattice constants (≥ 50 nm) are less accurate. Nevertheless, our tests show that the overall features in the wave functions are well converged.

In Fig. 4 (upper panels), we present several typical wave functions for a 1D nanotube array, with the lattice constant $d = 60$ nm and $k = 0$. The unit cell fills the $-d/2 < x < d/2$ and $-\infty < y < \infty$ strip, where the tube is placed at the origin. Like the two-tube states, wave functions in the 1D lattice have two parity quantum numbers, corresponding to reflections about the x and y axes. Many such states come in pairs, which become degenerate in a square 2D lattice, where they are connected by a $\pi/2$ rotation. This is the case of the state displayed in the left panel, antisymmetric along the $y = 0$ line, or the state with four angular nodes, in the middle panel. In the right panel, we display a state which is substantially *detached* from the tube surfaces, despite the fact that the orbit does not fit well in the elementary cell. This is remarkable, since the detachment for the two-tube states is largely lost already at much bigger separations, before the single-tube orbits of neigh-

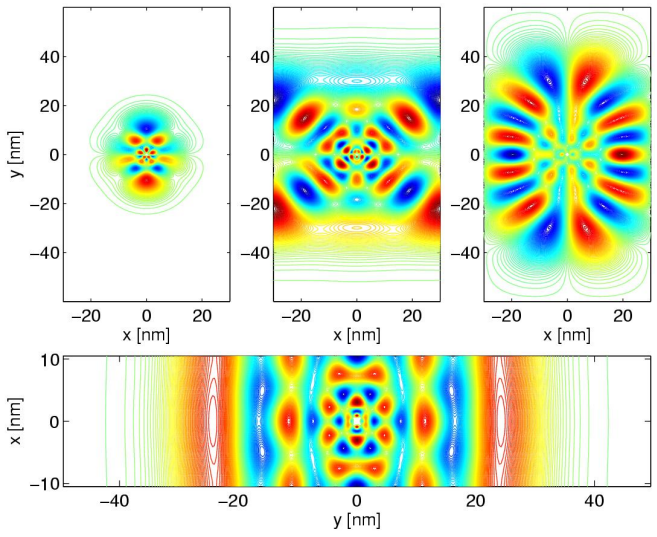

FIG. 4 (color online). Selected eigenstates of the periodic 1D array of nanotubes, described in the text.

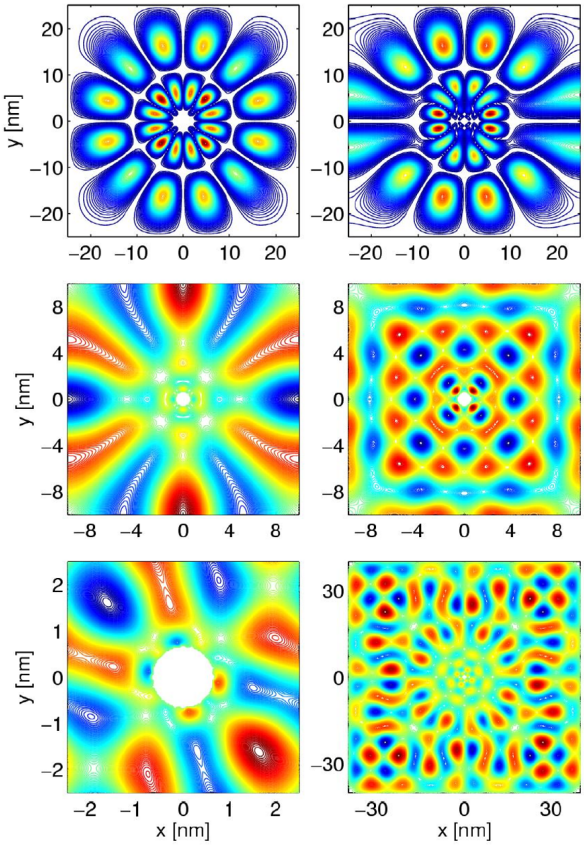

FIG. 5 (color online). Selected eigenstates of the periodic 2D lattice of nanotubes, described in the text.

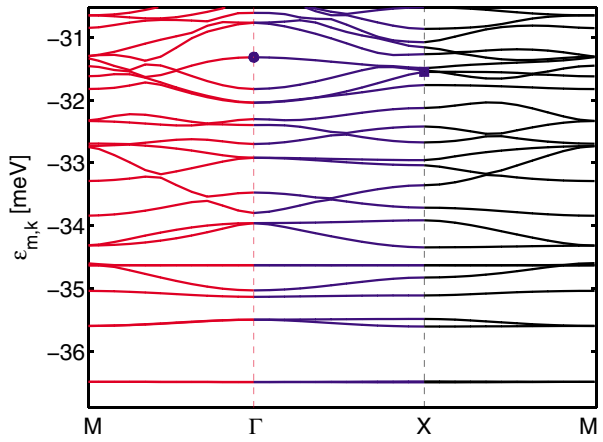

FIG. 6 (color online). The single-electron band structure of image states in the vicinity of a 2D array of nanotubes, with $d = 50$ nm. The boundaries are defined by the Γ [$\mathbf{k} = (k_x, k_y) = (0, 0)$], X [$\mathbf{k} = (\pi/d, 0)$], and M [$\mathbf{k} = (\frac{\pi}{d}, \frac{\pi}{d})$] points. We present the (50–73)rd bands. The square (circle) denotes the X (Γ) point of the 68th (70th) band, with probability densities of the states plotted in upper part of Fig. 5 right (left).

boring tubes even "touch" (see Fig. 3 middle left). This underlines the importance of periodicity for the preservation of detachment, where the *central character* of the attractive force at each tube is largely preserved by the presence of symmetrically placed neighboring tubes.

In general, higher excited states are separated further from the tubes and their structure is more complex. On the other hand, at separations larger than $\approx d$ the wave functions behave more like above a *flat plane*, as we show in the lower panel of Fig. 4, with $d = 20$ nm and axes rotated by $\pi/2$. The noncircular shape in the center appears here and in other pictures, due to the relatively coarse grid used. We can also study the k dependence of these Bloch states inside their bands.

Let us examine first the states in square 2D arrays of nanotubes, where the unit cell spans the region from $-d/2$ to $d/2$ on both axes. In Fig. 5, we display some pertinent 2D-wave functions. In the upper left panel, we show for $d = 50$ nm the probability density of a state, of an approximate $l = 6$ and $n = 2$ nodal counting, that is detached from the tubes' surfaces. It corresponds to the Γ point in Fig. 6. In contrast, as we move through the band to the X point, the state partially collapses on the tubes' surfaces (right panel). In the middle panels, we also display two wave functions for $d = 20$ nm. In the left panel, we show a ($l = 6$, $n = 1$) detached state, and in the right panel, we give a state with a nodal structure of a quartic symmetry. In the lower left and right panels, we display a diagonally aligned state for $d = 5$ nm and a detached state for $d = 80$ nm, respectively.

In Fig. 6, we present the single-electron bands for the 2D lattice of nanotubes, for $d = 50$ nm and $\Delta/d = 0.01$, calculated between the Γ, X, and M points. Some bands are degenerate at the Γ point, due to their symmetry with the $\pi/2$ rotation. The low-energy bands, corresponding to states highly localized around each tube, are very flat and well separated [see the (50–53)rd bands], so the associated *band gaps* can block propagation of the Rydberg electrons. Higher bands ($m > 60$) are broader and denser, so that band gaps disappear and avoided crossings emerge. The calculated band structure is quite well converged; i.e., by changing Δ/d from 0.01 to 0.007 the energies of the (50–74)th states changed by less than 0.5%. Besides the band-state energies, the TISs are also determined by their lifetimes, due to scattering on phonons and disorder in the nanotube array [8].

The TISs were recently observed in isolated nanotubes [9] and studies in nanotube arrays are in preparation. These Bloch states should be tunable by changing the nearest intertube separations d_i, since their energies scale roughly as $E \approx E_0 + \sum_i \alpha_i/d_i$. We anticipate their applications in guiding and storing of Rydberg-like electrons and for information processing.

This project was supported by the German-Israeli Foundation, the EU IHP program HPRN-CT-1999-00129, the U.S. National Science Foundation, the Office of Naval Research, the Feinberg graduate school, and through a grant to the Institute for Theoretical Atomic, Molecular and Optical Physics at the Harvard-Smithsonian Center for Astrophysics.

[1] P. Vukusic and J. R. Sambles, Nature (London) **424**, 852 (2003).
[2] J. D. Joannopoulos, P. R. Villeneuve, and S. Fan, Nature (London) **390**, 143 (1997); A. Chutinan, S. John, and O. Toader, Phys. Rev. Lett. **90**, 123901 (2003).
[3] P. R. Villeneuve and M. Piche, Phys. Rev. B **46**, 4973 (1992).
[4] K. Kempa *et al.*, Nano Lett. **3**, 13 (2003).
[5] M. P. A. Jones, C. J. Vale, D. Sahagun, B. V. Hall and E. A. Hinds, Phys. Rev. Lett. **91**, 080401 (2003).
[6] B. E. Granger, P. Král, H. R. Sadeghpour, and M. Shapiro, Phys. Rev. Lett. **89**, 135506 (2002).
[7] W. G. Scherzer, H. L. Selzle, E. W. Schlag and R. D. Levine, Phys. Rev. Lett. **72**, 1435 (1994).
[8] D. Segal, P. Král, and M. Shapiro, Chem. Phys. Lett. **392**, 314 (2004); (to be published).
[9] M. Zamkov *et al.*, Phys. Rev. Lett. **93**, 156803 (2004).
[10] Y. Homma *et al.*, Appl. Phys. Lett. **81**, 2261 (2002).
[11] M. P. Robinson, B. L. Tolra, Michael W. Noel, T. F. Gallagher, and P. Pillet, Phys. Rev. Lett. **85**, 4466 (2000).
[12] U. Höfer *et al.*, Science **277**, 1480 (1997).
[13] N. W. Ashcroft and N. D. Mermin, *Solid State Physics* (Saunders College Publishing, New York, 1976).
[14] S. Kanfer and M. Shapiro, J. Phys. Chem. **88**, 3964 (1984); D. T. Colbert and W. H. Miller, J. Chem. Phys. **96**, 1982 (1992); J. C. Light and T. Carrington, Adv. Chem. Phys. **114**, 263 (2000).